



Asymmetry and uncertainties in biogeophysical climate–vegetation feedback over a range of CO₂ forcings

M. Willeit, A. Ganopolski, and G. Feulner

Potsdam Institute for Climate Impact Research, Potsdam, Germany

Correspondence to: M. Willeit (willeit@pik-potsdam.de)

Received: 17 July 2013 – Published in Biogeosciences Discuss.: 7 August 2013

Revised: 27 November 2013 – Accepted: 28 November 2013 – Published: 3 January 2014

Abstract. Climate–vegetation feedback has the potential to significantly contribute to climate change, but little is known about its range of uncertainties. Here, using an Earth system model of intermediate complexity we address possible uncertainties in the strength of the biogeophysical climate–vegetation feedback using a single-model multi-physics ensemble. Equilibrium experiments with halving (140 ppm) and doubling (560 ppm) of CO₂ give a contribution of the vegetation–climate feedback to global temperature change in the range -0.3 to -0.1 °C and -0.1 to 0.2 °C, respectively. There is an asymmetry between warming and cooling, with a larger, positive vegetation–climate feedback in the lower CO₂ climate. Hotspots of climate–vegetation feedback are the boreal zone, the Amazon rainforest and the Sahara. Albedo parameterization is the dominant source of uncertainty in the subtropics and at high northern latitudes, while uncertainties in evapotranspiration are more relevant in the tropics. We analyse the separate impact of changes in stomatal conductance, leaf area index and vegetation dynamics on climate and we find that different processes are dominant in lower and higher CO₂ worlds. The reduction in stomatal conductance gives the main contribution to temperature increase for a doubling of CO₂, while dynamic vegetation is the dominant process in the CO₂ halving experiments. Globally the climate–vegetation feedback is rather small compared to the sum of the fast climate feedbacks. However, it is comparable to the amplitude of the fast feedbacks at high northern latitudes where it can contribute considerably to polar amplification. The uncertainties in the climate–vegetation feedback are comparable to the multi-model spread of the fast climate feedbacks.

1 Introduction

Vegetation distribution is controlled by climate, predominantly by temperature and precipitation (e.g. Holdridge, 1947; Köppen, 1936; Prentice et al., 1992). Vegetation structure is also influenced by the atmospheric CO₂ concentration, which affects photosynthesis and consequently the allocation of carbon to the different biomass pools. This can result in changes in physically relevant characteristics of the vegetation, such as the leaf area index (LAI) (e.g. McCarthy et al., 2007; Norby et al., 2005; Woodward, 1990). Increased CO₂ concentration has been shown to reduce stomatal conductance and thus lower evapotranspiration (e.g. Medlyn et al., 2001). The opposite effect has been observed for a CO₂ decrease (e.g. Brodribb et al., 2009).

Vegetation in turn influences climate through various physical and biochemical processes. On the one hand, changes in vegetation affect the fluxes of sensible and latent heat from the surface to the atmosphere, the amount of short-wave radiation absorbed by the surface and the exchange of momentum between the land surface and the air (e.g. Brovkin et al., 2009; Kleidon et al., 2000; Bala et al., 2007). On the other hand, vegetation changes are accompanied by changes in the vegetation and soil carbon content, which are associated with changes in surface–air fluxes of CO₂ and can alter the concentration of CO₂ in the atmosphere (e.g. Arneth et al., 2010; Cox et al., 2000; Friedlingstein et al., 2006; Schimel, 1995). The first kind of processes is referred to as biogeophysical, the second kind as biogeochemical. As a result of these interactions with climate, vegetation has the potential to amplify or dampen climate change and thus act as a positive or negative feedback on climate. In this study we focus only on the impact of vegetation on the

biogeophysical land surface–atmosphere processes and in the following when we refer to climate–vegetation feedback, we mean exclusively the biogeophysical part.

The sign and strength of the biogeophysical climate–vegetation feedback is the result of the combination of changes in different surface–atmosphere fluxes (i.e. of energy, water and momentum) which affect near-surface air temperature, possibly in opposite directions. The net effect of vegetation changes on climate will depend on the relative contribution of the single factors and will in general be a function of geographic location and time of the year (e.g. Bala et al., 2007).

Changes in CO₂ affect vegetation through its effect on plant physiology. Under higher CO₂, stomatal conductance is expected to decrease because plants open stomata less widely causing a reduction in the water vapour flux from the leaf interior to the surrounding air. This is confirmed both by free air CO₂-enrichment experiments and by modelling studies (e.g. Ainsworth and Rogers, 2007; Betts et al., 1997; Medlyn et al., 2001; Sellers et al., 1996), which suggest a reduction of stomatal conductance by around 20 % for a doubling of CO₂. The pure physiological effect of CO₂ on stomatal conductance in models has been shown to cause a decrease in evapotranspiration over land and consequently a global land surface warming of 0.2–0.5 °C (Betts et al., 1997; Boucher et al., 2008; Cao et al., 2010; Sellers et al., 1996). Reduction in stomatal conductance has caused a runoff increase during the last century (Gedney et al., 2006) and is projected to continue to do so into the future (Betts et al., 2007).

In a higher CO₂ world, photosynthesis by plants is expected to increase (even without climate change) if water and nutrients are not limiting (e.g. Ainsworth and Rogers, 2007; Owensby et al., 1999). Via this so-called CO₂ fertilisation effect, plants assimilate more carbon and are more productive if atmospheric CO₂ is higher. This will cause an increase in the LAI, which lowers surface albedo and increases evapotranspiration (e.g. Betts et al., 2000, 1997; Bonan et al., 1992). Higher CO₂ concentrations promote water-use efficiency of plants as the land biosphere can take up more CO₂ per unit of water loss. This mechanism would tend to favour forests over grasslands, because more biomass can be produced per unit water used. However, nutrients, particularly nitrogen, could be a strong limiting factor for CO₂ fertilisation (Reich et al., 2006; Vitousek and Howarth, 1991). Betts et al. (1997) showed that structural changes in vegetation, in particular increased LAI, could offset the warming caused by the reduced stomatal conductance.

Additional impacts of vegetation on climate come from changes in vegetation cover. The most studied aspect of it is the so-called “taiga–tundra” feedback. In northern high latitudes the extent of forest is limited mainly by temperature. As projected by climate models, temperature will increase in a higher CO₂ world with an amplification of the warming in high latitudes. There is a general agreement between models that this temperature increase will allow taiga forest to

expand northward and replace part of the tundra (Bala et al., 2006; Falloon et al., 2012; Levis et al., 1999; O’ishi and Abe-Ouchi, 2009; Port et al., 2012). On the one hand, the shift from tundra to forest significantly decreases surface albedo, especially in the presence of snow, causing surface air temperatures to rise due to the increased amount of absorbed solar radiation. On the other hand, the expansion of forests will also increase the evapotranspiration in these regions, resulting in an increase in latent heat flux, which cools the surface directly through evaporative cooling and indirectly through changes in cloud cover. The increase in roughness length will increase both latent and sensible heat fluxes through an increase in the drag coefficient for turbulent fluxes, assuming fixed atmospheric conditions (e.g. Garratt, 1977).

Different models generally agree on a positive vegetation–climate feedback in high northern latitudes where, for a CO₂ doubling, the decrease in albedo dominates over the increase in evapotranspiration resulting in a net annual warming due to northward forest expansion. Levis et al. (1999) find a land warming north of 45° N of about 1 °C and 0.5 °C in spring and summer, respectively, while they find a cooling in winter. Falloon et al. (2012) find annual warming larger than 1.5 °C over the same area.

Projected vegetation changes in a warmer climate are more uncertain in lower latitudes, where agreement between different models is worse (e.g. Sitch et al., 2008). Several modelling studies show that vegetation might be particularly sensitive to climate change in the Sahara and in the Amazon basin. There is evidence from both data and modelling studies that the Sahara was greener than today during the mid-Holocene when summer insolation in the Northern Hemisphere (NH) was higher and therefore the west-African monsoon stronger (Brovkin et al., 2002; Claussen et al., 1999; Doherty et al., 2000; Ganopolski et al., 1998; DeMenocal et al., 2000). In a 2 × CO₂ world, the standard CLIMBER-2 version simulates an expansion of grassland into about 10 % of the Sahara (Claussen et al., 2003). Future projections of the west-African monsoon by general circulation models (GCMs) which do not include vegetation dynamics do not agree on the sign of precipitation anomalies in the Sahel region (Cook and Vizzy, 2006). Some early studies with Earth system models (ESMs) point to the possibility of a dieback of the Amazon rainforest under global warming scenarios (Betts et al., 2004; Cox et al., 2000). This result is strongly model dependent and other studies simulate a minor or no reduction in Amazon forest cover (Levis et al., 2000; Port et al., 2012).

Altogether, significant uncertainties and intermodel variability exist on the amplitude and the sign of the biogeophysical vegetation–climate feedback for a CO₂ doubling in current ESMs. Values range from global temperature decrease by –0.1 °C (Betts et al., 2000) to an increase by 0.1–0.3 °C (Falloon et al., 2012; Jiang et al., 2011; Levis et al., 2000; Notaro et al., 2007). Uncertainties are even more pronounced on regional scales. Quantifying these uncertainties and the

responsible processes is fundamental for increasing the reliability of future climate projections on continental scales and for improving the understanding of the biosphere–climate interactions. The analysis of these uncertainties in climate–vegetation feedbacks is the first issue we address in this paper.

In addition to this uncertainty analysis, it is useful to compare the vegetation feedback with the fast climate feedbacks in a framework where different feedbacks can be compared in a consistent way. Unlike the classical Charney feedbacks – water vapour, cloud, lapse rate and albedo – which are considered to be “fast”, vegetation feedback is treated as “slow” and is therefore not included in the calculation of equilibrium climate sensitivity. However, it is considered of importance for the Earth system sensitivity which also invokes “slow” climate feedbacks, such as ice sheet, etc. (Hansen et al., 2008). In fact, different aspects of vegetation response to changing climate and CO₂ have different timescales ranging from years to centuries. For instance, the physiological effect of changes in CO₂ on stomatal conductance occurs on timescales from years to decades, while changes in the distribution of vegetation cover are an order of magnitude slower. The comparison of the vegetation feedback with fast climate feedbacks is the second issue discussed in the paper.

Finally, it is known that fast climate feedbacks are strongly model dependent (Bony et al., 2006; Soden and Held, 2006; Solomon et al., 2007) and that they can be also strongly climate state dependent (Colman and McAvaney, 2009; Crucifix, 2006; Yoshimori et al., 2011). The third issue we explore in this study is the state-dependence of the climate–vegetation feedback, in particular the asymmetry between colder and warmer climates induced by lower and higher CO₂ concentrations, respectively. The knowledge about asymmetry of climate feedbacks is crucial for the attempts to derive climate (and Earth system) sensitivity from past climates. It is reasonable to assume that not only the magnitude of the feedbacks can be state dependent but also their uncertainties. This is because different processes might be more or less important depending on the state of the system. As an example, larger areas are covered by snow in colder climates, therefore the uncertainties in the parameterization of snow related processes will result in larger uncertainties in a cold rather than in a warm climate. State dependence and uncertainties in the feedbacks are thus not fully decoupled but rather have to be considered together.

We use a multi-physics ensemble approach (Watanabe et al., 2012) in a single model framework to estimate the uncertainty range in the biogeophysical climate–vegetation feedback at global and continental scales. Single-model ensembles with perturbed physics are routinely used in climate modelling. However, it is generally believed that single model ensembles may considerably underestimate the range of uncertainties compared to multi-model ensembles due to lack of structural uncertainties (Yokohata et al., 2013). Here we make an attempt to overcome this deficiency of single-

model ensemble by changing, systematically, not only model parameters but also the structure of parameterizations of the relevant biogeophysical processes in a single model framework. Our multi-physics ensemble approach allows us to estimate magnitude and uncertainties in the climate–vegetation feedback and to compare them in a consistent framework with magnitudes and uncertainties of the fast climate feedbacks as reported in Soden and Held (2006) for different climate models.

We benefit from the use of an Earth system model of intermediate complexity (EMIC) which is highly computationally efficient and allows for a systematic analysis of the impact of changes in model structure on the biogeophysical climate–vegetation feedback. In this study we use a single and simplified vegetation model and we do not address the uncertainties that could arise from the use of different and possibly more comprehensive dynamic global vegetation models (DGVMs). The spread in modelled changes in vegetation distribution for future climate projections as projected by current DGVMs has been studied elsewhere (Sitch et al., 2008; Cramer et al., 2001).

2 Methodology

2.1 Model

For our analysis we use the Earth system model of intermediate complexity CLIMBER-2 (Ganopolski et al., 2001; Petoukhov et al., 2000). CLIMBER-2 includes a 2.5-D dynamical-statistical atmosphere and a multi-basin, zonally averaged ocean model including sea ice. It also includes VECODE, a dynamic model of the terrestrial biosphere (Brovkin et al., 1997, 2002). VECODE distinguishes three surface cover types: forest, grassland and desert. The vegetation distribution is determined only by temperature and precipitation. In general VECODE compares well with other dynamic global vegetation models for present-day climate (Cramer et al., 2001). The CO₂ fertilisation effect on net primary productivity (NPP) is explicitly considered in the model and thus CO₂ directly affects the LAI. NPP is increased by 25% for a CO₂ doubling and decreased by 25% for a halving of CO₂. However, unlike more complex DGVMs, NPP in VECODE does not directly affect fractions of plant functional types (trees, grass). This is a weakness of our model which has implications described below. The marine carbon cycle components are not used in this study. Atmospheric CO₂ is prescribed in all experiments and the potential atmospheric CO₂ changes due to changes in the land surface carbon pools are not considered.

2.2 Multi-physics ensemble

Here we use a multi-physics ensemble approach (Watanabe et al., 2012) in a single model framework to estimate the uncertainty range in the biogeophysical climate–vegetation

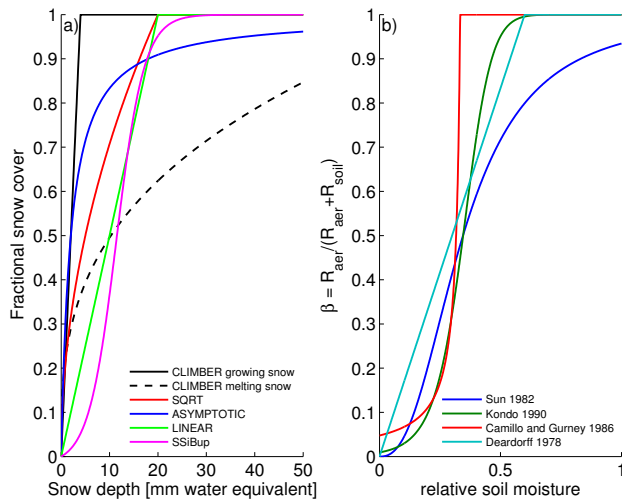


Fig. 1. Parameterizations of (a) subgrid snow cover fraction (Liston and Elder, 2004) and (b) surface resistance (Mahfouf and Noilhan, 1991). R_{soil} is the surface resistance and R_{aer} is the aerodynamic resistance to the transfer of water from the surface to a reference height, assumed to be 50 s m^{-1} . See text for further details.

feedback at global and continental scales. We consider structural uncertainties in sub-grid snow cover fraction, snow masking by vegetation, albedo and evapotranspiration, including stomatal and surface conductance. For all these processes we include several approaches found in the literature in CLIMBER-2 (Tables 1, 2).

2.2.1 Albedo

To account for subgrid heterogeneities, in most GCMs sub-grid snow cover fraction is parameterized as a function of grid-cell mean snow depth or snow mass (Liston and Elder, 2004). The relationship used between the grid-cell mean quantities and the snow cover fraction has a considerable impact on the modelled albedo of snow-covered areas. We use five different parameterizations for subgrid scale snow cover (Fig. 1a and Table 1). We prescribe bare soil albedo as being either a constant global value or prescribed from present-day observations. In both cases we also introduce a soil wetness dependence, following BATS (Dickinson et al., 1993).

Forests are very efficient in masking snow. In the presence of snow, surface albedo is significantly lower over forests than over grasslands. Indicative values of albedo for snow covered forests estimated from satellite data are around 0.2–0.3, while for grasslands and surfaces with short vegetation the albedo can be as high as 0.5–0.6 (Barlage et al., 2005; Bonan, 2008; Jin et al., 2002; Moody et al., 2007). In situ measurements show an even higher difference, with snow-covered albedos as low as 0.13 for forests and higher than 0.7 for grasslands (e.g. Betts and Ball, 1997). Several different approaches are used in state-of-the-art ESMs to parameterize snow masking by vegetation, which are generally

related to the surface albedo scheme used. We include two albedo schemes in CLIMBER-2. The first one is based on BATS (Dickinson et al., 1993) and computes the albedo as a weighted mean of snow-covered and snow-free vegetation albedo. The fraction covered by snow is a function of the roughness length and varies with surface types. The second, more complex albedo parameterization, is based on the JS-BACH scheme used in Otto et al. (2011). It uses the leaf and stem area index (LSAI) to determine the fraction of vegetated area which is given sub-canopy soil or vegetation (PFT specific) albedo. A value of 0.11–0.3 is assigned to the albedo of snow covered canopy. Additionally, for clear sky albedo, we augment the LSAI parameterization with a solar zenith angle dependence following Hellström (2000). The fraction of soil viewing the sky is not only a function of the stem area and the canopy density but also of the elevation of the sun above the horizon.

2.2.2 Evapotranspiration

In our ensemble we also include ensemble members with different representations of evapotranspiration, i.e. Penman–Monteith and an aerodynamic formulation based on the Monin–Obukhov similarity theory. The Monin–Obukhov similarity theory (Monin and Obukhov, 1954) relates turbulent surface–atmosphere water vapour flux to the difference of mean humidity at two levels in the constant-flux layer through the universal stability functions. The Penman–Monteith equation (Monteith, 1965; Penman, 1948) can be regarded as a physics-based combination of the available energy (Priestley and Taylor, 1972) and aerodynamic (Monin–Obukhov) approaches. The Penman–Monteith and the aerodynamic formulations are most frequently used in ESMs (Pitman et al., 1999).

In both approaches, the vegetation controls the exchange of water between the surface and the atmosphere through the resistance exerted by leaf stomata on the diffusion of water from inside the leaf to the atmosphere. Stomatal resistance is tightly coupled to the process of carbon assimilation through photosynthesis and in some ESMs it is modelled by the photosynthesis module. Alternative formulations of the stomatal resistance are based on empirical formulations, where stomatal resistance generally depends on environmental factors such as radiation, temperature, humidity and on soil moisture availability. Since CLIMBER-2 does not model photosynthesis explicitly we include several empirical formulations of the stomatal resistance in the model following Dickinson et al. (1993) and Stewart (1988). Stomatal resistance is also dependent on the CO_2 concentration in the atmosphere, as with higher CO_2 levels stomata need to open less to get the same amount of CO_2 into the leaf interior. CO_2 enrichment experiments have shown a decrease in stomatal conductance (inverse of stomatal resistance) for a doubling of environmental CO_2 concentration (Ainsworth and Rogers, 2007; Medlyn et al., 2001). Although they find that the amplitude

Table 1. Parameterizations for different biogeophysical processes included in the model ensemble.

Process	Parameterizations
Subgrid snow cover, Liston and Elder (2004)	Sqrt Asymptotic Linear SSIB
Snow masking by vegetation	BATS, Dickinson et al. (1993) ECHAM, Otto et al. (2011)
Evapotranspiration	Monin–Obukhov similarity theory, Monin and Obukhov (1954) Penman–Monteith, Penman (1948); Monteith (1965)
Stomatal conductance	BATS, Dickinson et al. (1993) Stewart, linear, Stewart (1988) Stewart, non-linear, Stewart (1988)
Surface resistance, Mahfouf and Noilhan (1991)	Sun (1982) Kondo (1990) Camillo and Gurney (1986) Deardorff (1978)

Table 2. Range of parameter values for different parameters affecting the biogeophysical processes included in the model ensemble.

Parameter	Range
Diffuse new snow albedo	0.85–0.95
Visible soil albedo, Dickinson et al. (1993)	0.1–0.2
Visible snow-covered canopy albedo	0.11–0.3
Height of snow that covers half of forest	0.3–1 m
Height of snow that covers half of grassland	0.05–0.2 m
Forest stem area index, Otto et al. (2011)	1–3 m ² m ⁻²
Minimum daily stomatal resistance	140–160 m s ⁻¹
Growing degree days for full phenology	200–400 gdd
Fraction of tree roots in the top 10 cm of soil	0.3–0.4
Fraction of grass roots in the top 10 cm of soil	0.45–0.55
Factor for CO ₂ dependence of stomatal conductance, Medlyn et al. (2001)	0.6–0.85

of the decrease in stomatal conductance varies largely between different species and with many other factors, they observe a mean long-term (after more than 1 yr of exposure of the plants to doubled CO₂) decrease of about 20%. In the model we introduced a range from 15–40% for the decrease in stomatal conductance for a CO₂ doubling, which is consistent with observations (Medlyn et al., 2001). Analogously, for CO₂ halving we increase stomatal conductance by 15–40%, although there is some evidence from data that the response might not be symmetric with respect to changes in CO₂ concentration and different species might react differently (Brodribb et al., 2009).

Over bare soils, where vegetation is not present, evaporation is largely controlled by water availability in the top soil layer. This limiting factor is accounted for through the introduction of a surface resistance. Four different parameterizations of the surface resistance are implemented into the model based on the work by Mahfouf and Noilhan (1991). Figure 1b shows the quantity $\beta = \frac{R_{\text{aer}}}{R_{\text{aer}} + R_{\text{soil}}}$ as a function of

the relative soil moisture in the top soil layer. R_{soil} is the surface resistance and R_{aer} is the aerodynamic resistance to the transfer of water from the surface to a reference height, assumed to be 50 s m⁻¹.

A more detailed description of the parameterizations used for the different processes is shown in Table 1. Additionally, to structural uncertainties we also explored the uncertainty due to parameters which are not well constrained by observations. A description of these parameters is listed in Table 2. Three values are sampled for each parameter, two at the limits and one in the middle of the range indicated in Table 2. Where no reference is added, the parameter range is estimated specifically for this study.

To construct the ensemble, we first created all possible permutations of parameters and parameterizations, which resulted in a large number of combinations. To reduce the number of ensemble members to a computationally manageable size, we randomly selected 250 sets of parameters and parameterizations. Then we run the 250 ensemble members

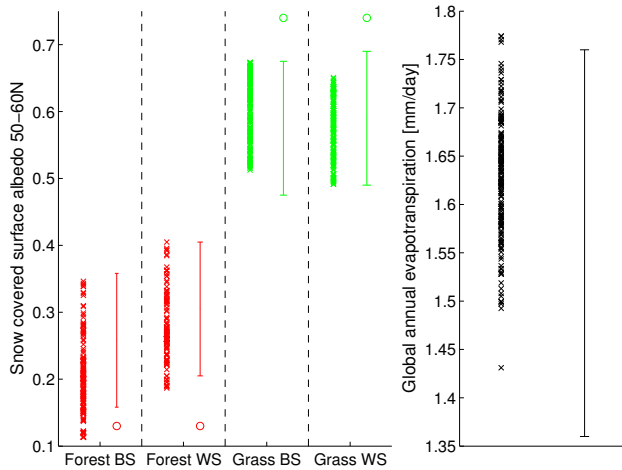


Fig. 2. (a) Comparison of the clear-sky (BS) and cloudy-sky (WS) albedo of snow covered forest and grass for all the ensemble members (crosses) with data from MODIS (error bar) (Jin et al., 2002; Moody et al., 2007). Circles indicate the albedo values from site observations (Betts and Ball, 1997). (b) Comparison of the mean annual evapotranspiration rate over land for all the ensemble members (crosses) and the reference data from (Mueller et al., 2011) (error bar).

to equilibrium for 6000 yr with present-day boundary conditions. We excluded ensemble members which were not compatible with observations of the albedo of snow covered forest and grassland and global land evapotranspiration (Fig. 2). This is essential, because these are two of the fundamental quantities determining the strength of the climate–vegetation feedback. In all, 145 ensemble members satisfied these criteria and constitute the final ensemble.

2.3 Forcings

We chose atmospheric CO₂ concentration as the external forcing on the Earth system as it is likely the most relevant radiative forcing for future climate. To cover a wide range of potential CO₂ concentrations we performed experiments with 140 ppm and 560 ppm, $\frac{1}{2} \times$ and $2 \times$ the preindustrial value (280 ppm), respectively. The choice of progressive CO₂ doubling is made because the radiative forcing of CO₂ is approximately logarithmic in its concentration. This set-up allows us to explore the state dependence of the climate–vegetation feedback.

2.4 Climate–vegetation feedback factor

A traditional way to quantify the interaction between vegetation and climate is to look at the feedback factor, similarly to what is traditionally done for the Charney feedbacks. The equilibrium surface temperature change due to changing CO₂ concentrations can be expressed as (Hansen and Taka-

hashi, 1984)

$$\Delta T_s = \frac{\lambda_0}{1 - \lambda_0 \sum F_j} \text{RF}, \quad (1)$$

where RF is the radiative forcing due to CO₂ concentration change, λ_0 is the Stefan–Boltzmann response,

$$\lambda_0 = - \left(\frac{\partial R_{\text{TOA}}}{\partial T_s} \right)^{-1} \quad (2)$$

and F_j are the feedback factors:

$$F_j = \frac{\partial R_{\text{TOA}}}{\partial V_j} \frac{\partial V_j}{\partial T_s}, \quad (3)$$

where R_{TOA} is the radiative balance at the top of the atmosphere (TOA), V is a vector of the internal climate variables which depend on temperature and affect the radiative balance at TOA through either or both short-wave (SW) and long-wave (LW) radiation. Additionally to the standard fast feedbacks (i.e. water vapour, cloud, albedo, lapse rate) here we also include vegetation, which will affect R_{TOA} through the different albedo of diverse vegetation types and changes in water vapour and clouds caused by changes in evapotranspiration. What we call here “albedo feedback” is the standard Charney feedback which does not include albedo changes due to shifts in vegetation zones.

Different methods have been applied in the past to quantify the feedbacks F_j of a given climate model (Cess et al., 1990; Soden et al., 2004; Wetherald and Manabe, 1988). Here we apply the offline TOA radiation method, which has been pioneered by Wetherald and Manabe (1988). It is based on the direct calculation of the radiative perturbation at TOA resulting from a substitution of one climate variable V_j from perturbed experiments at a time in the control runs, keeping all the other variables fixed. This quantity, normalised by the change in global mean temperature, can then be taken as a direct measure of the feedback strength of the variable V_j .

It should be stressed here that, compared to the fast feedbacks, vegetation changes occur on timescales of decades to centuries. Since in this study we focus on equilibrium conditions rather than transient behaviour of the climate system, the equal treatment of vegetation and Charney feedbacks is justified.

2.5 Experiments

With the described modelling set-up we performed different equilibrium experiments: (a) *C* – a control experiment with interactive vegetation and a preindustrial CO₂ concentration of 280 ppm; experiments with CO₂ at 140 and 560 ppm; (b) *R* – only the radiative effect of CO₂ doubling or halving on climate with all vegetation properties prescribed from the control; (c) *RP* – experiments different from *R* by including the physiological effect of CO₂ on stomatal conductance but not changing LAI and vegetation type; (d) *RPL* – same as *RP*

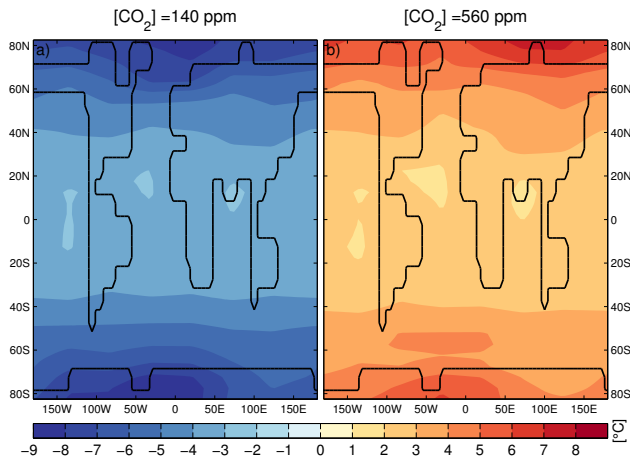


Fig. 3. Ensemble-mean annual temperature anomalies relative to the preindustrial climate ($R-C$) for (a) $\frac{1}{2} \times \text{CO}_2$ and (b) $2 \times \text{CO}_2$ for experiments with prescribed vegetation from the control. All values are significant at the 95 % level.

but including also the effect of CO_2 fertilisation on LAI; and (e) RPLV – the same as RPL but allowing vegetation cover to adjust to the changed climatic conditions. This set-up allows one to disentangle the impact of the different vegetation processes on climate. The experiments are outlined in Table 3. All experiments were run to equilibrium for 6000 model years using the preindustrial climate state as initial condition. The mean variables over the last 1000 yr of simulation are used in the analysis.

Additionally, to determine the strength of the climate–vegetation feedback in terms of the instantaneous radiative imbalance at the TOA, we run the control simulations again, substituting vegetation from the control run with vegetation simulated in RPLV experiments and computing the radiative imbalance at TOA. With the same procedure, but from R experiments, we also determined the strength of the traditional fast (Charney) feedbacks: water vapour, clouds, lapse rate and albedo (without changes in vegetation).

3 Results and discussion

3.1 Experiments with fixed vegetation: $R-C$

Figure 3 illustrates modelled climate changes relative to preindustrial under different atmospheric CO_2 with prescribed vegetation from the control runs. The global mean temperature changes are (median (5% value, 95% value)) $\Delta T_{\frac{1}{2} \times} = -3.2$ ($-3.3, -3.1$) $^{\circ}\text{C}$, $\Delta T_{2 \times} = 2.9$ ($2.9, 3.0$) $^{\circ}\text{C}$ for halving and doubling of CO_2 , respectively, which is close to equilibrium climate sensitivity of the standard CLIMBER-2 model version. The fact that the values $\Delta T_{\frac{1}{2} \times}$ and $\Delta T_{2 \times}$ are not equal points to the existence of weak non-linearities in

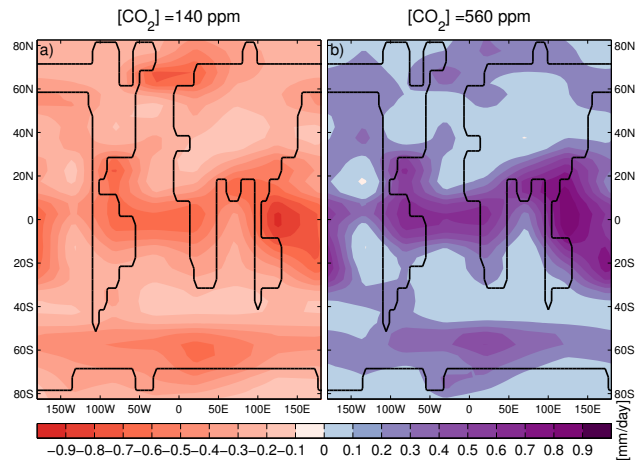


Fig. 4. Ensemble-mean annual precipitation anomalies relative to the preindustrial climate ($R-C$) for (a) $\frac{1}{2} \times \text{CO}_2$ and (b) $2 \times \text{CO}_2$ for experiments with prescribed vegetation from the control. All values are significant at the 95 % level.

the climate feedbacks in the model. The temperature anomalies are amplified in high latitudes (Fig. 3a and b).

Analogously, for global precipitation, $\Delta P_{\frac{1}{2} \times} = -0.28$ ($-0.27, -0.29$) mm day^{-1} and $\Delta P_{2 \times} = 0.29$ ($0.28, 0.3$) mm day^{-1} . Precipitation changes relative to preindustrial are located mainly in the tropics (Fig. 4a and b).

3.2 The effect of interactive vegetation

In the following we discuss the effects of vegetation on climate by adding new processes step-by-step. All results refer to differences from the radiative only (R) experiment. We start from the physiological effect of CO_2 on stomatal conductance, then we add the CO_2 fertilisation effect on LAI and finally we include the impact of dynamic vegetation and discuss the total combined effect of vegetation on climate.

3.2.1 CO_2 physiological effect: RP-R

The prescribed reduction in stomatal conductance by 15–40 % due to the pure physiological effect of CO_2 doubling causes a warming of 0.1 (0.05, 0.3) $^{\circ}\text{C}$ over land (Fig. 5a). This is consistent with previous modelling results (Betts et al., 1997; Cao et al., 2010; Sellers et al., 1996), although it is close to the lower range of values from these studies. Evapotranspiration over land is reduced by -0.1 ($-0.05, -0.3$) mm day^{-1} (Fig. 5d), which is higher than was found in most previous studies (e.g. Cao et al., 2010). As a consequence the hydrological cycle is weakened and precipitation over land is reduced by about 0.1 mm day^{-1} . Warming is particularly significant where evapotranspiration is important, such as in the tropics and in NH mid-latitudes with values higher than 0.5 $^{\circ}\text{C}$ in the Amazon region (Fig. 6b). The warming is caused by a reduced surface latent heat flux and more

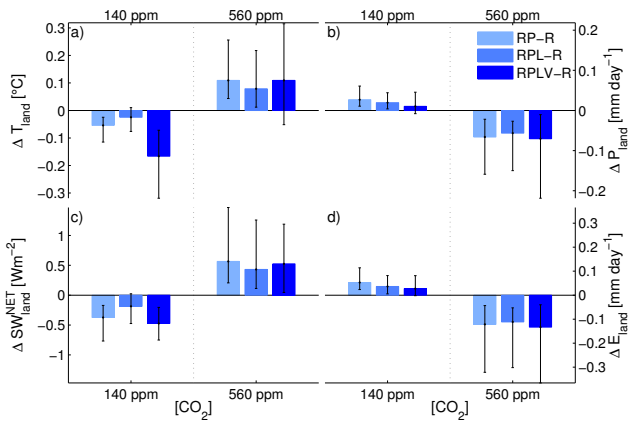


Fig. 5. Global annual land anomalies of (a) surface air temperature, (b) precipitation, (c) net short-wave radiation at the surface and (d) evapotranspiration for RP, RPL and RPLV experiments. All anomalies are relative to the *R* experiment which considers only the radiative effect of CO₂. Shown are the median and the 5–95 percentile range of the ensemble.

short-wave radiation absorbed at the surface due to less cloud cover (Fig. 5c–d). The effect of cloud cover changes dominates in the boreal zone, while the weaker latent heat flux is more important in the tropics. All ensemble members consistently show a warming in the tropics and the NH (Fig. 7b).

In the simulations with 140 ppm, the CO₂ physiological effect results in a widespread but small cooling over land of less than 0.1 °C due to enhanced evapotranspiration (Figs. 5a, 6a and 7a).

3.2.2 CO₂ fertilisation on LAI: RPL-*R*

As a response to enhanced CO₂ the LAI increases everywhere, predominantly at mid-latitudes where a zonal mean increase in growing-season peak LAI of up to 1 m⁻² is modelled (Fig. 8c). Higher LAI enhances evapotranspiration and partially offsets the reduction in evapotranspiration due to closing stomata, dampening the surface warming caused by the physiological effect of CO₂, particularly over NH land (Figs. 5a and 6d). This is in qualitative agreement with the results of Betts et al. (1997), although they found a stronger cooling effect of increased LAI. The difference can at least partly be explained by the much larger increase in LAI in their model, also because they implicitly included changes in LAI from shifts in vegetation cover. Global land precipitation and evapotranspiration are only slightly increased (Fig. 5b and d). The impact of increased LAI on surface albedo plays only a secondary role.

In the 140 ppm experiments, the LAI decreases by more than 1 m² m⁻² in mid-latitudes. This causes a warming which almost completely offsets the small cooling caused by higher stomatal conductance (Figs. 5a, 6c and 7a).

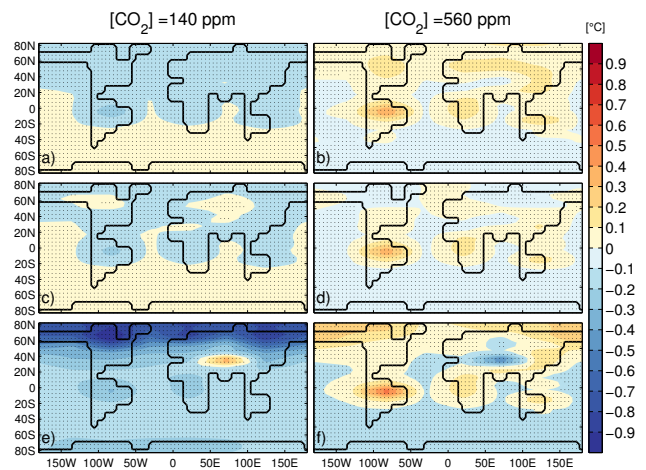


Fig. 6. Ensemble mean annual temperature anomalies relative to *R* for RP (top), RPL (middle) and RPLV (bottom) experiments for CO₂ of 140 ppm (left) and 560 ppm (right). Dots indicate areas where values are significant at the 95 % level.

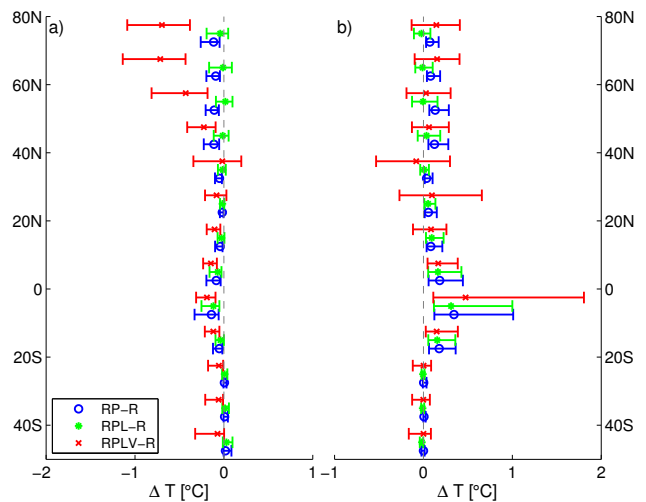


Fig. 7. Zonal annual land temperature anomalies relative to *R* for RP (blue), RPL (green) and RPLV (red) experiments for CO₂ of 140 ppm (a) and 560 ppm (b). Shown are the median and the 5–95 percentile range of the ensemble.

3.2.3 Dynamic vegetation: RPLV-*R*

Modelled vegetation distribution changes substantially as a response to changing climatic conditions in both higher and lower CO₂ worlds. Anomalies of vegetation cover with respect to preindustrial are shown in Fig. 8. In the warmer climate simulations with 560 ppm of CO₂, forest cover increases significantly in high northern latitudes and decreases in mid-latitudes. The modelled response to a colder climate (140 ppm) is the opposite, but not fully symmetric to warming. Simulated changes in forest fractions in the high latitudes correspond to a northward (southward) treeline

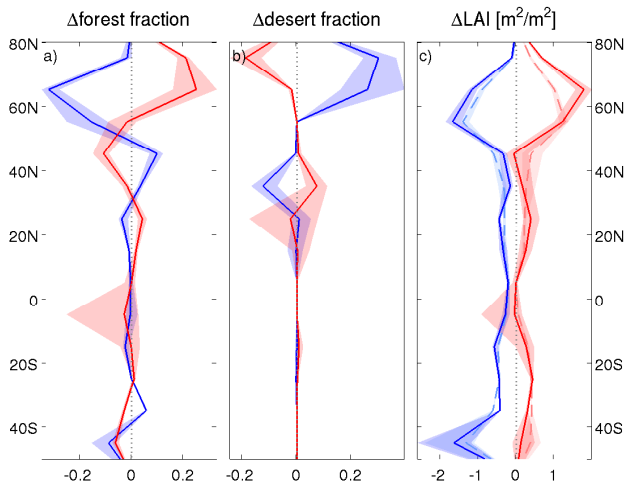


Fig. 8. Zonal forest, desert and LAI anomalies relative to preindustrial for experiments with fully interactive vegetation (RPLV). CO₂ of 140 ppm (blue) and 560 ppm (red). Solid lines indicate the median and the shading represents the 5–95 percentile range of the ensemble. For LAI also the anomalies for the RPL experiment are shown (dashed lines). LAI anomalies are computed from values in the peak growing season.

migration by ≈ 300 km for $2\times\text{CO}_2$ ($\frac{1}{2}\times\text{CO}_2$). The change in tropical forest is strongly dependent on the model structure, with the main contribution to uncertainties coming from the equatorial South America. The parameterization of stomatal conductance is the dominant factor explaining this uncertainty, with higher reductions in forest cover simulated in the ensemble members using the linear model from Stewart (1988). The forest changes for $\frac{1}{2}\times\text{CO}_2$ are approximately symmetric to those for warmer climates, except for the tropics, where no significant changes are modelled.

Desert changes are substantial in high northern latitudes where the desert fraction decreases with increasing CO₂ concentrations. Moreover, desert anomalies are significant in the NH subtropics, where desert expands in warmer climates and retracts in colder climates (Fig. 8b). The “greening” of the Sahara is the most uncertain aspect. Here the parameterization of soil albedo gives the main contribution to the uncertainty range.

Forest expansion in high northern latitudes for higher CO₂ concentrations is consistent with previous modelling results (Notaro et al., 2007; O’ishi and Abe-Ouchi, 2009; Port et al., 2012; Lucht et al., 2006; Bala et al., 2006). The greening of the Sahara in projections of future climate with higher CO₂ levels is seen in some models. In transient simulations with the RCP8.5 scenario, Port et al. (2012) found an initial decrease in the desert fraction over the Sahel/Sahara region, followed by an increase around the end of the 21st century. O’ishi and Abe-Ouchi (2009) found an expansion of vegetation in the Sahel/Sahara region for doubling and quadrupling of CO₂.

Amazon forest dieback under global warming is a feature of some models (Betts et al., 2004; Cox et al., 2000; Huntingford et al., 2008). Other models simulate a more modest reduction in forest cover (Port et al., 2012). O’ishi and Abe-Ouchi (2009) found no significant change in the Amazon forest in a $2\times\text{CO}_2$ climate. This broad range of model behaviours is well represented in our ensemble.

In the fully interactive vegetation runs, changes in LAI are the result of the combined effects of CO₂ fertilisation and response of vegetation distribution to climate change. Zonal mean LAI is increased by forest expansion in high northern latitudes and decreased by forest retreat in mid-latitudes and in the Amazon region (Fig. 8c). For $\frac{1}{2}\times\text{CO}_2$ the impact of dynamic vegetation on zonal LAI is a reduction between 50–70° N due to a southward retreat of forest and an increase between 30–40° N due to an expansion of forest.

Vegetation dynamics act as a positive feedback on climate in most ensemble members amplifying the warming in $2\times\text{CO}_2$ and the cooling in $\frac{1}{2}\times\text{CO}_2$ experiments. With a CO₂ of 140 ppm, vegetation dynamics is the main contributor to the total cooling caused by vegetation, while for CO₂ doubling the contribution is only minor (Fig. 5a). Dynamic vegetation is very important in high latitudes in the CO₂ halving simulations, where it causes significant additional cooling, up to 1 °C in the zonal annual mean (Figs. 6e and 7a). Additionally it causes warming (cooling) over central Asia in the 140 ppm (560 ppm) experiments due to a reduction (increase) in desert area (Fig. 6e and f), mainly because of surface albedo changes.

For both $\frac{1}{2}\times\text{CO}_2$ and $2\times\text{CO}_2$, vegetation dynamics enhance the uncertainty range relative to the RPL-R experiments everywhere (Figs. 5a and 7a and b), because the way the biogeophysical processes are parameterized influences the shifts in vegetation cover.

When considering this finding one should keep in mind that the vegetation distribution in VECODE is not affected by changes in NPP, but only by temperature and precipitation. Thus, although we implicitly account for an increase in water use efficiency because for increased CO₂ NPP is increasing and stomata are closing, this does not affect the distribution of vegetation. The expansion of forest in our model might thus be underestimated in CO₂ doubling experiments.

3.2.4 Total effect of vegetation on climate

Asymmetry

The global land temperature differences between the simulations with interactive vegetation and those with prescribed preindustrial vegetation are $\Delta T_{\frac{1}{2}\times}^{\text{veg}} = -0.2$ (−0.05, −0.3) °C and $\Delta T_{2\times}^{\text{veg}} = 0.1$ (−0.05, 0.3) °C (Fig. 5a). Globally, the climate–vegetation feedback is larger in the 140 ppm than in the 560 ppm climate. Two simple considerations can explain this asymmetric behaviour, which is determined mainly by asymmetries in the boreal zone (Fig. 7). First, the albedo

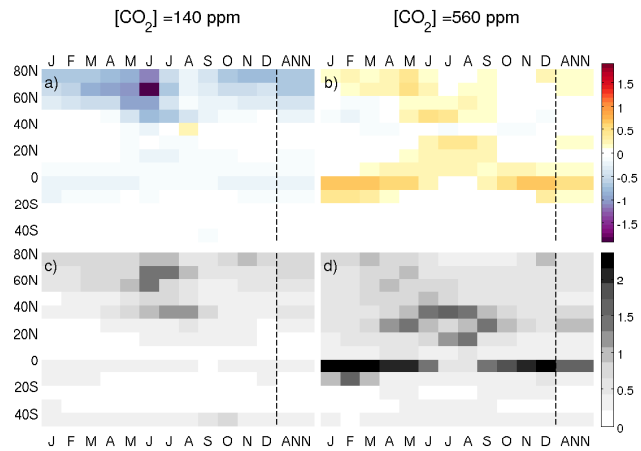


Fig. 9. Zonal mean near-surface land–air temperature differences between fully interactive (RPLV) and fixed (*R*) vegetation runs as a function of latitude and season for experiments with 140 ppm (left) and 560 ppm (right). Shown are the median (top) and the 5–95 percentile range (bottom) of the ensemble. Annual mean zonal values are also shown on the right of each panel.

increase for CO₂ halving is larger than the albedo decrease for CO₂ doubling because snow in the NH extends further south in the colder climate, thus enhancing the changes in albedo due to vegetation cover shifts. Second, there is a higher potential of southward vegetation retreat compared to the northward vegetation expansion in warmer climates because the area of tundra and polar desert are already small for the preindustrial climate.

The impact of vegetation changes on climate varies as a function of latitude and season (Fig. 9a–b). In the 140 ppm case, vegetation has the biggest impact on temperature in high northern latitudes. At latitudes higher than about 40–50° N vegetation acts as a positive feedback amplifying the cooling, particularly in spring, when snow masking by forests is important (Fig. 9).

For doubling of CO₂, vegetation changes cause significant warming of about 1 °C over the tropics throughout the year (Fig. 9b). This is a consequence of the reduced evapotranspiration due to the reduced stomatal conductance, combined with a reduction in forest over the Amazon in some ensemble members. North of 40° N, warming of up to 1 °C is modelled during spring and summer and cooling, around –0.5 °C, during winter. At 20° N a warming is found because of Sahara “greening” and at 30° N a cooling because of larger desert fraction in central Asia.

The changes in surface air temperature due to vegetation changes are the result of the combined effect of variations in several biogeophysical processes controlling the surface energy balance. Albedo and evapotranspiration changes are the two dominant effects. A transition from grass to forest, or an increase in LAI, increases the short-wave radiation absorbed by the surface through a lowering of the surface albedo. This

Table 3. Experiments description.

Experiment	CO ₂	Vegetation set-up
<i>C</i>	280 ppm	fully interactive
<i>R</i>	140 ppm 560 ppm	prescribed from <i>C</i>
RP	140 ppm 560 ppm	CO ₂ effect on stomatal conductance LAI prescribed from <i>C</i> vegetation cover prescribed from <i>C</i>
RPL	140 ppm 560 ppm	CO ₂ effect on stomatal conductance CO ₂ effect on LAI vegetation cover prescribed from <i>C</i>
RPLV	140 ppm 560 ppm	CO ₂ effect on stomatal conductance CO ₂ effect on LAI dynamic vegetation

effect will be particularly strong when snow is present, because of the strong snow masking effect of forests. On the other hand, more water is evaporated and transpired from forests as compared to grass. This will increase the latent heat flux and thus cool the surface. Changes in evapotranspiration also affect atmospheric water content and cloudiness that also affect surface air temperature. The relative contribution of albedo and evapotranspiration to surface temperature change varies as a function of latitude and season (Fig. 10). To quantify when and where each of the two effects dominates, we computed for each latitude and each month the correlation between the zonal mean near-surface air temperature and both evapotranspiration and albedo in the ensemble. We first excluded insignificant and unphysical (positive) correlations and then, for each latitude and month of the year, we chose the highest value between the temperature–evapotranspiration correlation and the temperature–albedo correlation. We changed sign of the correlation coefficient of temperature with evapotranspiration and sum the two fields to obtain a metric between –1 and 1, with –1 indicating perfect correlation of temperature with albedo and +1 perfect correlation of temperature with evapotranspiration. The result shows that evapotranspiration has the dominant effect on temperature in the tropics and albedo is more important in the subtropics for both halving and doubling of CO₂ (Fig. 10). In the 140 ppm experiments the albedo effect dominates throughout the year also north of 50° N. For CO₂ doubling, north of 40° N the albedo is more important in spring and winter, but the evapotranspiration effect dominates in summer. This helps interpreting the seasonal temperature variations in Fig. 9.

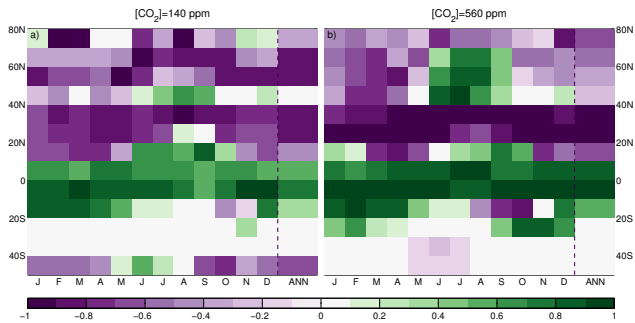


Fig. 10. Representation of the relative importance of albedo and evapotranspiration changes due to vegetation changes to surface air temperature anomalies over land as a function of latitude and season. Green shading indicates that evapotranspiration and purple shading that the albedo effect is dominant in determining temperature anomalies. See text for further explanation on how this metric is computed.

Uncertainties

Not only are the mean ensemble values of the climate–vegetation feedback state-dependent, but so are the uncertainties. In general uncertainties in the boreal zone are dominant in the 140 ppm climate, while uncertainties in the tropics and subtropics are more important in the 560 ppm climate (Figs. 7 and 9c–d).

In the 140 ppm experiments the uncertainty is largest in the high northern latitudes (Fig. 9c), with values as high as the signal itself. In this region the main contribution to the uncertainty range comes from the representation of the snow masking by vegetation and is largest in spring/early summer, when snow is still on the ground and insolation is increasing, so that surface albedo becomes important. Minor uncertainties are found in the subtropics, because of an uncertain retreat of desert in central Asia.

In the 560 ppm experiments, major uncertainties, higher than 100 %, are found around 5° S, mainly because of the Amazon rain-forest dieback in some ensemble members, and between 20–30° N because of the uncertain “greening” of the Sahara and expansion of desert in central Asia (Fig. 9d). The uncertainties over the Amazon are an indirect effect of the impact of different evapotranspiration parameterizations on the fate of the rain-forest, which has the main control on the changes in evaporative surface cooling. Over desert regions, the parameterizations of both surface albedo and evapotranspiration influence the degree to which desert expands in central Asia and retreats over the Sahara in a warming climate. Significant uncertainties are found also north of 60° N in spring and are attributable to the snow masking parameterization.

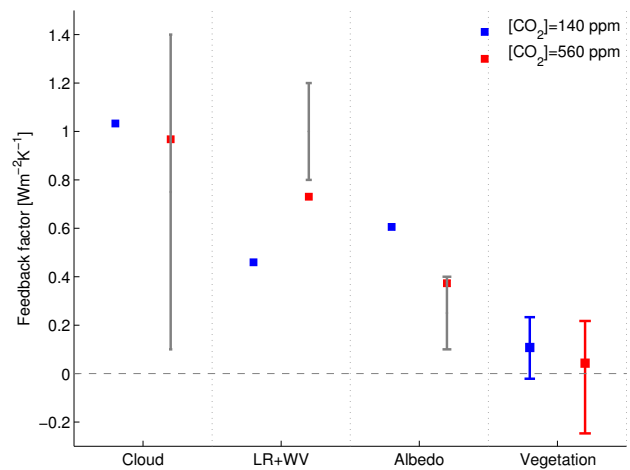


Fig. 11. Global feedback factors for cloud, lapse rate (LR) plus water vapour (WV), albedo and vegetation for experiments with 140 ppm (blue), and 560 ppm (red). The filled squares indicate the ensemble median. For the vegetation feedback, the bars show the range from the ensemble. For the fast feedbacks, the errorbars represent the inter-model range from the AR4 models from Soden and Held (2006).

3.3 Climate–vegetation feedback factor

The feedback factor approach allows one to directly compare the vegetation feedback with the Charney feedbacks. The global feedback factors for the experiments with different CO₂ concentrations are shown in Fig. 11. The fast feedbacks for doubling of CO₂ can be compared with the results from GCMs (Soden and Held, 2006). The vegetation feedback is globally relatively small. For CO₂ doubling it covers the range from -0.2 to $+0.2$ $\text{W m}^{-2} \text{K}^{-1}$. The ensemble mean is very close to zero. Climate–vegetation feedback is positive for CO₂ halving with values up to 0.2 $\text{W m}^{-2} \text{K}^{-1}$ and higher. The uncertainty in the global climate–vegetation feedback for CO₂ doubling is similar to the inter-model spread in the fast climate feedbacks (Fig. 11).

The vegetation feedback is comparable with the other feedbacks in high northern latitudes, while it is close to zero elsewhere, even if significant differences exist between different ensemble members (Fig. 12a). For both CO₂ concentrations the vegetation feedback is positive in high northern latitudes but slightly negative in mid-latitudes with major uncertainties in the subtropics (Fig. 12b), especially for CO₂ doubling.

There is a reasonably high correlation between the global vegetation feedback factor and global mean temperature change due to vegetation feedback (Fig. 13). The linear relation is valid for both halving and doubling of CO₂ and has approximately the same slope in both cases. The vegetation feedback factor is thus a robust measure of the strength of the climate–vegetation feedback, at least at global scale.

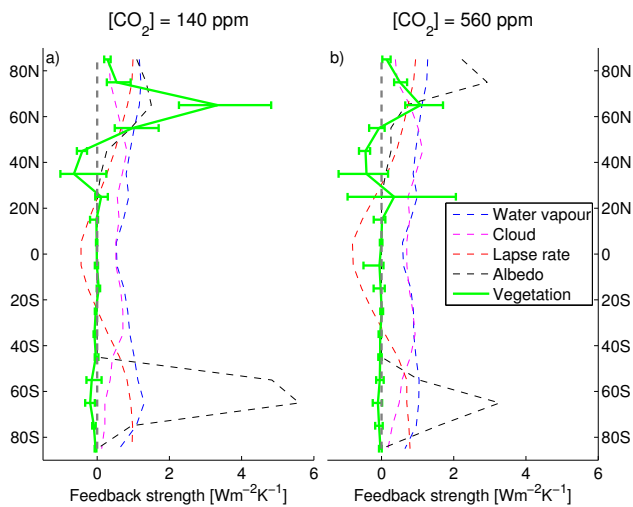


Fig. 12. Zonal mean feedback strength for experiments with 140 ppm (left) and 560 ppm (right). The ensemble median is plotted for all feedbacks and the 5–95 percentile range from the ensemble is additionally plotted for the vegetation feedback.

The range in the magnitude of the vegetation–climate feedback presented here originates only from the uncertainties in biogeophysical land–atmosphere processes. Additional uncertainties would come from the response of vegetation cover to climate which is not represented in our study, because we use a single vegetation model. On a more fundamental level the uncertainty range would also be affected by the strength of the fast climate feedbacks (i.e. the climate sensitivity), which in our study covers only a small portion of the possible range estimated from data and different models. Considering also these factors could lead to an even larger uncertainty range in vegetation–climate feedback, thus our estimates can be regarded as conservative.

4 Conclusions

Using a multi-physics ensemble we studied the uncertainties in the strength of the biogeophysical vegetation–climate feedback. We find that uncertainties are in many cases larger than the signal itself.

For CO₂ doubling, there is not even an agreement on the sign of the global vegetation feedback between ensemble members. A step-by-step analysis of different vegetation processes shows evidence that a large part of the uncertainties comes from the response to vegetation shift. A robust warming of 0.1 (0.05, 0.3) °C over land is modelled due to a CO₂ induced reduction in stomatal conductance and, as the result, reduced transpiration. The increased LAI slightly reduces this warming in all ensemble members. Allowing vegetation to adjust to the new climatic conditions results in an increase of the uncertainties and a total effect of vegetation on temperature over land of 0.1 (−0.05, 0.3) °C. This

value is reduced to essentially zero if the global mean temperature is considered. Nevertheless we find that vegetation causes an ensemble mean annual warming over the Amazon of 0.5 °C with values up to 2 °C in some ensemble members exhibiting rainforest dieback in this region. In northern mid- and high latitudes vegetation amplifies the seasonal cycle by about 1 °C through warming in spring–summer and cooling in winter. Major uncertainties arise from the forest reduction in the Amazon region and the Sahara “greening” in some ensemble members.

For CO₂ halving, the vegetation feedback is found to be robustly positive with an enhanced cooling over land of −0.2 (−0.05, −0.3) °C. The main contribution comes from the high northern latitudes and is caused by an albedo increase due to southward retreat of the treeline. Globally, vegetation causes the temperature to decrease by a median value of −0.2 °C, which is less than 10 % of climate sensitivity. The physiological effect of lower CO₂ and the decrease in LAI have only a minor effect on surface air temperature.

A comparison of vegetation feedback in terms of radiative imbalance at the top of the atmosphere with the traditional fast climate feedbacks shows a globally small contribution of vegetation feedback. Consistently with vegetation induced changes in global temperature we find that the vegetation feedback factor is slightly positive for CO₂ halving and varies around a median value of zero for CO₂ doubling. However, at high northern latitudes vegetation feedback is comparable or even more important than the fast feedbacks, particularly in the 140 ppm experiments. The uncertainty in the vegetation–climate feedback is comparable to the inter-model spread in the fast climate feedbacks.

Our results demonstrate that there is an asymmetry in the vegetation–climate feedback between higher and lower CO₂ worlds and that changes in different vegetation processes affect climate in very different ways in CO₂ induced warmer and colder climate. The physiological effect of CO₂ on plants is shown to be most important in elevated CO₂ climates, while the effect of changes in climate on vegetation distribution is the dominant factor in climates colder than pre-industrial. This highlights the need for caution when using past glacial climate change to derive Earth system sensitivity applicable for future climate change.

In this work we explore only part of the uncertainties affecting the strength of the vegetation–climate feedback. Additional uncertainties will arise from, for example, the dynamic vegetation model itself and the climate sensitivity. Better observational constraints on the choice of parameters and parameterizations of biogeophysical processes are required to reduce the uncertainty range.

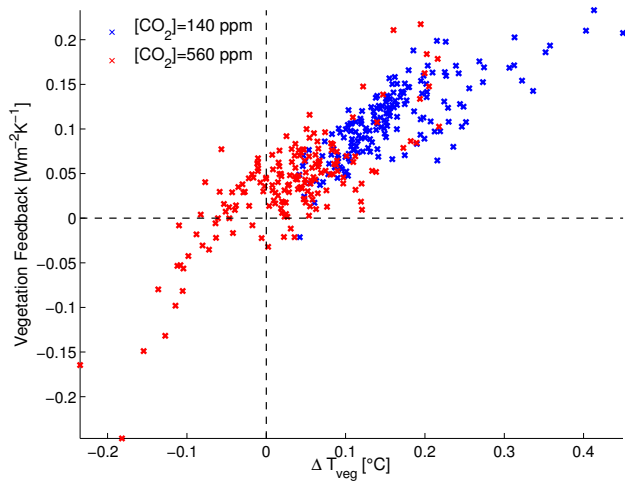


Fig. 13. Global vegetation feedback factor vs. global temperature difference between interactive and prescribed vegetation experiments ($\Delta T_{\text{veg}} = T_{\text{RPLV}} - T_{\text{R}}$) for all ensemble members. Red crosses represent the experiments with 560 ppm and blue crosses those with 140 ppm. The sign of ΔT_{veg} is reversed in the 140 ppm case to allow a direct comparison with the 560 ppm case. In reality ΔT_{veg} values are negative for all ensemble members in the 140 ppm experiments. A positive vegetation feedback indicates a vegetation induced global cooling for CO_2 halving and a global warming for CO_2 doubling.

Acknowledgements. The research leading to these results has received funding from the European Community's Seventh Framework Programme (FP7 2007-2013) under grant agreement no. 238366. The authors thank V. Brovkin for valuable comments, M. Flechsig for advice on the use of the SimEnv simulation environment and T. Schneider von Deimling for help with the feedback analysis. M. W. thanks D. Dalmonch for useful discussions. The authors thank G. Bala and an anonymous reviewer for constructive comments which helped improve the paper.

Edited by: P. Cox

References

- Ainsworth, E. A., and Rogers, A.: The response of photosynthesis and stomatal conductance to rising $[\text{CO}_2]$: mechanisms and environmental interactions, *Plant Cell Environ.*, 30, 258–270, doi:10.1111/j.1365-3040.2007.01641.x, 2007.
- Arnth, A., Harrison, S. P., Zaehle, S., Tsigaridis, K., Menon, S., Bartlein, P. J., Feichter, J., Korhola, A., Kulmala, M., O'Donnell, D., Schurgers, G., Sorvari, S., and Vesala, T.: Terrestrial biogeochemical feedbacks in the climate system, *Nat. Geosci.*, 3, 525–532, doi:10.1038/ngeo905, 2010.
- Bala, G., Caldeira, K., Mirin, A., Wickert, M., Delire, C., and Phillips, T. J.: Biogeophysical effects of CO_2 fertilization on global climate, *Tellus B*, 58, 620–627, doi:10.1111/j.1600-0889.2006.00210.x, 2006.
- Bala, G., Caldeira, K., Wickert, M., Phillips, T. J., Lobell, D. B., Delire, C., and Mirin, A.: Combined climate and carbon-cycle

- effects of large-scale deforestation., *P. Natl. Aca. Sci. USA*, 104, 6550–6555, doi:10.1073/pnas.0608998104, 2007.
- Barlage, M., Zeng, X., Wei, H., and Mitchell, K. E.: A global 0.05° maximum albedo dataset of snow-covered land based on MODIS observations, *Geophys. Res. Lett.*, 32, L17405, doi:10.1029/2005GL022881, 2005.
- Betts, A. K. and Ball, J. H.: Albedo over the boreal forest, *J. Geophys. Res.*, 102, 28901, doi:10.1029/96JD03876, 1997.
- Betts, R., Cox, P., Lee, S., and Woodward, F.: Contrasting physiological and structural vegetation feedbacks in climate change simulations, *Nature*, 387, 2–5, 1997.
- Betts, R., Cox, P., and Woodward, F.: Simulated responses of potential vegetation to doubled CO_2 climate change and feedbacks on near surface temperature, *Global Ecol. Biogeogr.*, 9, 171–180, 2000.
- Betts, R. A., Cox, P. M., Collins, M., Harris, P. P., Huntingford, C., and Jones, C. D.: The role of ecosystem-atmosphere interactions in simulated Amazonian precipitation decrease and forest dieback under global climate warming, *Theor. Appl. Climatol.*, 78, 157–175, doi:10.1007/s00704-004-0050-y, 2004.
- Betts, R. a., Boucher, O., Collins, M., Cox, P. M., Falloon, P. D., Gedney, N., Hemming, D. L., Huntingford, C., Jones, C. D., Sexton, D. M. H., and Webb, M. J.: Projected increase in continental runoff due to plant responses to increasing carbon dioxide, *Nature*, 448, 1037–1041, doi:10.1038/nature06045, 2007.
- Bonan, G. B.: Forests and climate change: forcings, feedbacks, and the climate benefits of forests, *Science*, 320, 1444–1449, doi:10.1126/science.1155121, 2008.
- Bonan, G. B., Pollard, D., and Thompson, S. L.: Effects of boreal forest vegetation on global climate, *Nature*, 359, 716–718, doi:10.1038/359716a0, 1992.
- Bony, S., Colman, R., Kattsov, V. M., Allan, R. P., Bretherton, C. S., Dufresne, J.-L., Hall, A., Hallegatte, S., Holland, M. M., Ingram, W., Randall, D. A., Soden, B. J., Tselioudis, G., and Webb, M. J.: How well do we understand and evaluate climate change feedback processes?, *J. Climate*, 19, 3445–3482, doi:10.1175/JCLI3819.1, 2006.
- Boucher, O., Jones, A., and Betts, R. A.: Climate response to the physiological impact of carbon dioxide on plants in the Met Office Unified Model HadCM3, *Clim. Dynam.*, 32, 237–249, doi:10.1007/s00382-008-0459-6, 2008.
- Brodribb, T. J., McAdam, S. A. M., Jordan, G. J., and Feild, T. S.: Evolution of stomatal responsiveness to CO_2 and optimization of water-use efficiency among land plants, *New Phytol.*, 183, 839–847, doi:10.1111/j.1469-8137.2009.02844.x, 2009.
- Brovkin, V., Ganopolski, A., and Svirezhev, Y.: A continuous climate–vegetation classification for use in climate-biosphere studies, *Ecol. Model.*, 101, 251–261, 1997.
- Brovkin, V., Bendtsen, J. R., Claussen, M., Ganopolski, A., Kutzbach, C., Petoukhov, V., and Andreev, A.: Carbon cycle, vegetation, and climate dynamics in the Holocene: experiments with the CLIMBER-2 model, *Global Biogeochem. Cy.*, 16, 1–20, doi:10.1029/2001GB001662, 2002.
- Brovkin, V., Raddatz, T., Reick, C. H., Claussen, M., and Gayler, V.: Global biogeophysical interactions between forest and climate, *Geophys. Res. Lett.*, 36, L07405, doi:10.1029/2009GL037543, 2009.
- Cao, L., Bala, G., Caldeira, K., Nemani, R., and Ban-Weiss, G.: Importance of carbon dioxide physiological forcing to future

- climate change., *P. Natl. Acad. Sci. USA*, 107, 9513–9518, doi:10.1073/pnas.0913000107, 2010.
- Cess, R. D., Potter, G. L., Blanchet, J. P., Boer, G. J., Del Genio, A. D., Déqué, M., Dymnikov, V., Galin, V., Gates, W. L., Ghan, S. J., Kiehl, J. T., Lacis, A. A., Le Treut, H., Li, Z.-X., Liang, X.-Z., McAvaney, B. J., Meleshko, V. P., Mitchell, J. F. B., Morcrette, J.-J., Randall, D. A., Rikus, L., Roeckner, E., Royer, J. F., Schlese, U., Sheinin, D. A., Slingo, A., Sokolov, A. P., Taylor, K. E., Washington, W. M., Wetherald, R. T., Yagai, I., and Zhang, M.-H.: Intercomparison and interpretation of climate feedback processes in 19 atmospheric general circulation models, *J. Geophys. Res.*, 95, 16601, doi:10.1029/JD095iD10p16601, 1990.
- Claussen, M., Kubatzki, C., Brovkin, V., Ganopolski, A., Hoelzmann, P., and Pachur, H.-J.: Simulation of an abrupt change in Saharan vegetation in the Mid-Holocene, *Geophys. Res. Lett.*, 26, 2037–2040, doi:10.1029/1999GL900494, 1999.
- Claussen, M., Brovkin, V., Ganopolski, A., Kubatzki, C., and Petoukhov, V.: Climate change in Northern Africa: the past is not the future, *Climatic Change*, 57, 99–118, doi:10.1023/A:1022115604225, 2003.
- Colman, R. and McAvaney, B.: Climate feedbacks under a very broad range of forcing, *Geophys. Res. Lett.*, 36, 1–5, doi:10.1029/2008GL036268, 2009.
- Cook, K. H. and Vizy, E. K.: Coupled model simulations of the West African monsoon system: twentieth- and twenty-first-century simulations, *J. Climate*, 19, 3681–3703, doi:10.1175/JCLI3814.1, 2006.
- Cox, P. M., Betts, R. A., Jones, C. D., Spall, S. A., and Totterdell, I. J.: Acceleration of global warming due to carbon-cycle feedbacks in a coupled climate model, *Nature*, 408, 184–187, doi:10.1038/35041539, 2000.
- Cramer, W., Bondeau, A., Woodward, F. I., Prentice, I. C., Betts, R. a., Brovkin, V., Cox, P. M., Fisher, V., Foley, J. a., Friend, A. D., Kucharik, C., Lomas, M. R., Ramankutty, N., Sitch, S., Smith, B., White, A., and Young-Molling, C.: Global response of terrestrial ecosystem structure and function to CO₂ and climate change: results from six dynamic global vegetation models, *Glob. Change Biol.*, 7, 357–373, doi:10.1046/j.1365-2486.2001.00383.x, 2001.
- Crucifix, M.: Does the Last Glacial Maximum constrain climate sensitivity?, *Geophys. Res. Lett.*, 33, L18701, doi:10.1029/2006GL027137, 2006.
- DeMenocal, P., Ortiz, J., Guilderson, T., Adkins, J., Sarnthein, M., Baker, L., and Yarusinsky, M.: Abrupt onset and termination of the African Humid Period, *Quaternary Sci. Rev.*, 19, 347–361, doi:10.1016/S0277-3791(99)00081-5, 2000.
- Dickinson, R. E., Henderson-Sellers, A., and Kennedy, P. J.: Biosphere-Atmosphere Transfer Scheme (BATS) version 1e as coupled to the NCAR community climate model. Technical note, Tech. rep., NCAR (National Center for Atmospheric Research), 1993.
- Doherty, R., Kutzbach, J., Foley, J., and Pollard, D.: Fully coupled climate/dynamical vegetation model simulations over Northern Africa during the mid-Holocene, *Clim. Dynam.*, 16, 561–573, doi:10.1007/s003820000065, 2000.
- Falloon, P. D., Dankers, R., Betts, R. A., Jones, C. D., Booth, B. B., and Lambert, F. H.: Role of vegetation change in future climate under the A1B scenario and a climate stabilisation scenario, using the HadCM3C Earth system model, *Biogeosciences*, 9, 4739–4756, doi:10.5194/bg-9-4739-2012, 2012.
- Friedlingstein, P., Cox, P., Betts, R., Bopp, L., von Bloh, W., Brovkin, V., Cadule, P., Doney, S., Eby, M., Fung, I., Bala, G., John, J., Jones, C., Joos, F., Kato, T., Kawamiya, M., Knorr, W., Lindsay, K., Matthews, H. D., Raddatz, T., Rayner, P., Reick, C., Roeckner, E., Schnitzler, K.-G., Schnur, R., Strassmann, K., Weaver, A. J., Yoshikawa, C., and Zeng, N.: Climate–carbon cycle feedback analysis: results from the C4MIP model intercomparison, *J. Climate*, 19, 3337–3353, doi:10.1175/JCLI3800.1, 2006.
- Ganopolski, A., Kubatzki, C., Claussen, M., Brovkin, V., and Petoukhov, V.: The influence of vegetation-atmosphere-ocean interaction on climate during the mid-Holocene, *Science*, 280, 1916–1919, doi:10.1126/science.280.5371.1916, 1998.
- Ganopolski, A., Petoukhov, V., Rahmstorf, S., Brovkin, V., Claussen, M., Eliseev, A., and Kubatzki, C.: CLIMBER-2: a climate system model of intermediate complexity. Part II: model sensitivity, *Clim. Dynam.*, 17, 735–751, doi:10.1007/s003820000144, 2001.
- Garratt, J. R.: Review of drag coefficients over oceans and continents, *Mon. Weather Rev.*, 105, 915–929, doi:10.1175/1520-0493, 1977.
- Gedney, N., Cox, P. M., Betts, R. A., Boucher, O., Huntingford, C., and Stott, P. A.: Detection of a direct carbon dioxide effect in continental river runoff records, *Nature*, 439, 835–838, doi:10.1038/nature04504, 2006.
- Hansen, J. E. and Takahashi, T. (Eds.): *Climate Processes and Climate Sensitivity*, vol. 29, Geophysical Monograph Series, American Geophysical Union, Washington DC, doi:10.1029/GM029, 1984.
- Hansen, J. E., Sato, M., and Kharecha, P.: Target atmospheric CO₂: where should humanity aim?, *Open Atmospheric Science Journal*, 2, 217–231, 2008.
- Hellström, R.: Forest cover algorithms for estimating meteorological forcing in a numerical snow model, *Hydrol. Process.*, 14, 3239–3256, doi:10.1002/1099-1085(20001230)14, 2000.
- Holdridge, L. R.: Determination of world plant formations from simple climatic data, *Science*, 105, 367–368, doi:10.1126/science.105.2727.367, 1947.
- Huntingford, C., Fisher, R. A., Mercado, L., Booth, B. B. B., Sitch, S., Harris, P. P., Cox, P. M., Jones, C. D., Betts, R. A., Malhi, Y., Harris, G. R., Collins, M., and Moorcroft, P.: Towards quantifying uncertainty in predictions of Amazon “dieback”, *Philos. T. Roy. Soc. B*, 363, 1857–1864, doi:10.1098/rstb.2007.0028, 2008.
- Jiang, D., Zhang, Y., and Lang, X.: Vegetation feedback under future global warming, *Theor. Appl. Climatol.*, 106, 211–227, doi:10.1007/s00704-011-0428-6, 2011.
- Jin, Y., Schaaf, C.B., Gao, F., Li, X., and Strahler, A. H.: How does snow impact the albedo of vegetated land surfaces as analyzed with MODIS data?, *Geophys. Res. Lett.*, 29, 1374, doi:10.1029/2001GL014132, 2002.
- Kleidon, A., Fraedrich, K., and Heimann, M.: A green planet versus a desert world: estimating the maximum effect of vegetation on the land surface climate, *Clim. Change*, 44, 471–493, 2000.
- Köppen, W.: *Das Geographische System Der Klimate*, W. Köppen und R. Geiger, Graz, München, 1936.

- Levis, S., Foley, J. A., and Pollard, D.: Potential high-latitude vegetation feedbacks on CO₂ – induced climate change, *Geophys. Res. Lett.*, 26, 747–750, doi:10.1029/1999GL900107, 1999.
- Levis, S., Foley, J. A., and Pollard, D.: Large-scale vegetation feedbacks on a doubled CO₂ climate, *J. Climate*, 13, 1313–1325, doi:10.1175/1520-0442(2000)013<1313:LSVFOA>2.0.CO;2, 2000.
- Liston, G. E. and Elder, K.: Representing subgrid snow cover heterogeneities in regional and global models, *J. Climate*, 17, 1381–1397, doi:10.1175/1520-0442(2004)017<1381:RSSCHI>2.0.CO;2, 2004.
- Lucht, W., Schaphoff, S., Erbrecht, T., Heyder, U., and Cramer, W.: Terrestrial vegetation redistribution and carbon balance under climate change, *Carbon Balance and Management*, 1, 6 pp., doi:10.1186/1750-0680-1-6, 2006.
- Mahfouf, J. and Noilhan, J.: Comparative study of various formulations of evaporations from bare soil using in situ data, *J. Appl. Meteorol.*, 30, 1354–1365, 1991.
- McCarthy, H. R., Oren, R., Finzi, A. C., Ellsworth, D. S., Kim, H.-S., Johnsen, K. H., and Millar, B.: Temporal dynamics and spatial variability in the enhancement of canopy leaf area under elevated atmospheric CO₂, *Glob. Change Biol.*, 13, 2479–2497, doi:10.1111/j.1365-2486.2007.01455.x, 2007.
- Medlyn, B. E., Barton, C. V. M., Broadmeadow, M. S. J., Ceulemans, R., De Angelis, P., Forstreuter, M., Freeman, M., Jackson, S. B., Kellomaki, S., Laitat, E., Rey, A., Roberntz, P., Sigurdsson, B. D., Strassmeyer, J., Wang, K., Curtis, P. S., and Jarvis, P. G.: Stomatal conductance of forest species after long-term exposure to elevated CO₂ concentration: a synthesis, *New Phytol.*, 149, 247–264, doi:10.1046/j.1469-8137.2001.00028.x, 2001.
- Monin, A. and Obukhov, A.: Basic laws of turbulent mixing in the surface layer of the atmosphere, *Contrib. Geophys. Inst. Acad. Sci.*, 24, 163–187, 1954.
- Monteith, J. L.: Evaporation and environment, *Sym. Soc. Exp. Biol.*, 19, 205–234, 1965.
- Moody, E. G., King, M. D., Schaaf, C. B., Hall, D. K., and Platnick, S.: Northern Hemisphere five-year average (2000–2004) spectral albedos of surfaces in the presence of snow: statistics computed from Terra MODIS land products, *Remote Sens. Environ.*, 111, 337–345, doi:10.1016/j.rse.2007.03.026, 2007.
- Mueller, B., Seneviratne, S. I., Jimenez, C., Corti, T., Hirschi, M., Balsamo, G., Ciais, P., Dirmeyer, P., Fisher, J. B., Guo, Z., Jung, M., Maignan, F., McCabe, M. F., Reichle, R., Reichstein, M., Rodell, M., Sheffield, J., Teuling, A. J., Wang, K., Wood, E. F., and Zhang, Y.: Evaluation of global observations-based evapotranspiration datasets and IPCC AR4 simulations, *Geophys. Res. Lett.*, 38, L06402, doi:10.1029/2010GL046230, 2011.
- Norby, R. J., Delucia, E. H., Gielen, B., Calfapietra, C., Gardina, C. P., King, J. S., Ledford, J., McCarthy, H. R., Moore, D. J. P., Ceulemans, R., De Angelis, P., Finzi, A. C., Karnosky, D. F., Kubiske, M. E., Lukac, M., Pregitzer, K. S., Scarascia-Mugnozza, G. E., Schlesinger, W. H., and Oren, R.: Forest response to elevated CO₂ is conserved across a broad range of productivity., *P. Natl. Acad. Sci. USA*, 102, 18052–18056, doi:10.1073/pnas.0509478102, 2005.
- Notaro, M., Vavrus, S., and Liu, Z.: Global vegetation and climate change due to future increases in CO₂ as projected by a fully coupled model with dynamic vegetation, *J. Climate*, 20, 70–90, doi:10.1175/JCLI3989.1, 2007.
- O’ishi, R. and Abe-Ouchi, A.: Influence of dynamic vegetation on climate change arising from increasing CO₂, *Clim. Dynam.*, 33, 645–663, doi:10.1007/s00382-009-0611-y, 2009.
- Otto, J., Raddatz, T., and Claussen, M.: Strength of forest-albedo feedback in mid-Holocene climate simulations, *Clim. Past*, 7, 1027–1039, doi:10.5194/cp-7-1027-2011, 2011.
- Owensby, C. E., Ham, J. M., Knapp, A. K., and Auen, L. M.: Biomass production and species composition change in a tallgrass prairie ecosystem after long-term exposure to elevated atmospheric CO₂, *Glob. Change Biol.*, 5, 497–506, doi:10.1046/j.1365-2486.1999.00245.x, 1999.
- Penman, H. L.: Natural evaporation from open water, bare soil and grass, *P. Roy. Soc. A-Math. Phys.*, 193, 120–145, doi:10.1098/rspa.1948.0037, 1948.
- Petoukhov, V., Ganopolski, A., Brovkin, V., Claussen, M., Eliseev, A., Kubatzki, C., and Rahmstorf, S.: CLIMBER-2: a climate system model of intermediate complexity. Part I: model description and performance for present climate, *Clim. Dynam.*, 16, 1–17, doi:10.1007/PL00007919, 2000.
- Pitman, A. J., Henderson-Sellers, A., Desborough, C. E., Yang, Z.-L., Abramopoulos, F., Boone, A., Dickinson, R. E., Gedney, N., Koster, R., Kowalczyk, E., Lettenmaier, D., Liang, X., Mahfouf, J.-F., Noilhan, J., Polcher, J., Qu, W., Robock, A., Rosenzweig, C., Schlosser, C. A., Shmakin, A. B., Smith, J., Suarez, M., Verseghy, D., Wetzell, P., Wood, E., and Xue, Y.: Key results and implications from phase 1(c) of the Project for Intercomparison of Land-surface Parametrization Schemes, *Clim. Dynam.*, 15, 673–684, doi:10.1007/s003820050309, 1999.
- Port, U., Brovkin, V., and Claussen, M.: The influence of vegetation dynamics on anthropogenic climate change, *Earth Syst. Dynam.*, 3, 233–243, doi:10.5194/esd-3-233-2012, 2012.
- Prentice, I., Cramer, W., and Harrison, S.: A global biome model based on plant physiology and dominance, soil properties and climate, *J. Biogr.*, 19, 117–134, 1992.
- Priestley, C. and Taylor, R.: On the assessment of surface heat flux and evaporation using large-scale parameters, *Mon. Weather Rev.*, 100, 81–92, 1972.
- Reich, P. B., Hobbie, S. E., Lee, T., Ellsworth, D. S., West, J. B., Tilman, D., Knops, J. M. H., Naeem, S., and Trost, J.: Nitrogen limitation constrains sustainability of ecosystem response to CO₂, *Nature*, 440, 922–925, doi:10.1038/nature04486, 2006.
- Schimel, D. S.: Terrestrial ecosystems and the carbon cycle, *Glob. Change Biol.*, 1, 77–91, 1995.
- Sellers, P. J., Bounoua, L., Collatz, G. J., Randall, D. A., Dazlich, D. A., Los, S. O., Berry, J. A., Fung, I., Tucker, C. J., Field, C. B., and Jensen, T. G.: Comparison of radiative and physiological effects of doubled atmospheric CO₂ on climate, *Science*, 271, 1402–1406, doi:10.1126/science.271.5254.1402, 1996.
- Sitch, S., Huntingford, C., Gedney, N., Levy, P. E., Lomas, M., Piao, S. L., Betts, R., Ciais, P., Cox, P., Friedlingstein, P., Jones, C. D., Prentice, I. C., and Woodward, F. I.: Evaluation of the terrestrial carbon cycle, future plant geography and climate-carbon cycle feedbacks using five Dynamic Global Vegetation Models (DGVMs), *Glob. Change Biol.*, 14, 2015–2039, doi:10.1111/j.1365-2486.2008.01626.x, 2008.

- Soden, B. and Held, I.: An assessment of climate feedbacks in coupled ocean-atmosphere models, *J. Climate*, 19, 3354–3360, 2006.
- Soden, B. J., Broccoli, A. J., and Hemler, R. S.: On the use of cloud forcing to estimate cloud feedback, *J. Climate*, 17, 3661–3665, 2004.
- Solomon, S., Manning, D., Chen, Z., Marquis, M., Averyt, K., Tignor, M., and Miller, H.: IPCC, Climate Change 2007, The Physical Science Basis, Fourth Assessment Report, 2007.
- Stewart, J.: Modelling surface conductance of pine forest, *Agr. Forest Meteorol.*, 43, 19–35, 1988.
- Vitousek, P. and Howarth, R.: Nitrogen limitation on land and in the sea: how can it occur?, *Biogeochemistry*, 13, 87–115, doi:10.1007/BF00002772, 1991.
- Watanabe, M., Shiogama, H., Yokohata, T., Kamae, Y., Yoshimori, M., Ogura, T., Annan, J. D., Hargreaves, J. C., Emori, S., and Kimoto, M.: Using a multiphysics ensemble for exploring diversity in cloud–shortwave feedback in GCMs, *J. Climate*, 25, 5416–5431, doi:10.1175/JCLI-D-11-00564.1, 2012.
- Wetherald, R. and Manabe, S.: Cloud feedback processes in a general circulation model, *J. Atmos.*, 45, 1397–1415, 1988.
- Woodward, F. I.: Global change: translating plant ecophysiological responses to ecosystems., *Trends Ecol. Evol.*, 5, 308–311, doi:10.1016/0169-5347(90)90087-T, 1990.
- Yokohata, T., Annan, J. D., Collins, M., Jackson, C. S., Shiogama, H., Watanabe, M., Emori, S., Yoshimori, M., Abe, M., Webb, M. J., and Hargreaves, J. C.: Reliability and importance of structural diversity of climate model ensembles, *Clim. Dynam.*, 1–19, doi:10.1007/s00382-013-1733-9, 2013.
- Yoshimori, M., Hargreaves, J. C., Annan, J. D., Yokohata, T., and Abe-Ouchi, A.: Dependency of feedbacks on forcing and climate state in physics parameter ensembles, *J. Climate*, 24, 6440–6455, doi:10.1175/2011JCLI3954.1, 2011.